

SCIENTIFIC REPORTS



OPEN

Hypoxia imaging in cells and tumor tissues using a highly selective fluorescent nitroreductase probe

Dan Yang¹, Hang Yu Tian², Tie Nan Zang¹, Ming Li², Ying Zhou¹ & Jun Feng Zhang³

Hypoxia is a characteristic of locally advanced solid tumors, resulting from an imbalance between oxygen consumption and supply. In hypoxic solid tumors, an increased expression of nitroreductase (NTR) is detected, therefore, the development of NTR-targeted fluorescent probes to selectively and efficiently detect hypoxia *in vivo* is of utmost importance. In this study, a probe (1) has been designed and tested for effective optical detection of NTR *in vitro* and *in vivo*. The reduction of probe (1), catalyzed by NTR, resulted in changes of the electron-withdrawn nitrogen group into an electron-donation amino group. In addition, breakage of the O-C bond ensured selective fluorescence enhancement. The *in vitro* response towards exogenous NTR, from rat liver microsomes, resulted in the optical enhancement during the detection process. *In vivo* imaging of caenorhabditis elegans (*C. elegans*) further confirmed the detection of NTR by probe (1). Moreover, probe (1) was successfully used for the detection of hypoxia in both HI5 cells, and a murine tumor model, which demonstrates the potential of probe (1) for application in fluorescence bioimaging studies, and tumor hypoxia diagnosis.

Nitroreductases (NTRs) are a family of flavin-containing enzymes that catalyze the reduction of nitroaromatic compounds to the corresponding amines using either NADH or NADPH as a source of reducing equivalents^{1,2}. NTRs play important roles in the bioremediation and degradation of toxicity of organic nitrogen compounds mediated by bacteria³. Under hypoxic conditions, overexpression of intracellular reductases, including NTRs, DT-diaphorase, and azoreductase was observed⁴. In solid tumors, expression of NTRs is directly related to the hypoxic status. Therefore, our goal was to measure hypoxia in tumor cells or tumor-derived tissue⁵⁻⁷.

Fluorescence imaging is a promising approach for monitoring bioactive molecules in living systems⁸⁻¹¹. Fluorescence imaging is a sensitive, selective, rapid, and an efficient bioanalytical tool for tracing the state, changes, and activities of targets *in vivo*, thereby facilitating progress in the fields of cell biology, and imaging using therapeutics¹²⁻¹⁶. Recently, the development of sensors that detect NTRs have attracted much attention because of their potential to detect the hypoxic status of a tumor¹⁷⁻²⁰. In these newly generated fluorescent probes, a selective 'switch' mechanism is used. The large electronic change resulting from the conversion of the electron-withdrawn nitro group to the electron-donation amino group leads to breakage of the O (or N)-C bond, which ensures recovery of the fluorescence signal and an 'off-on' recognition strategy. In addition, this reaction-based sensing mechanism guarantees that the probes have high selectivity towards NTRs. However, *in vivo* applications of NTR probes for selective imaging, and therapy of intracellular hypoxia are challenging. Given its promising properties, nitrobenzyl redox switching for NTR active materials was chosen as a preferred detection signal for the design of our NTR-switchable probe. We hypothesized that the probe could monitor intracellular hypoxic levels, and be used to investigate the relation between the hypoxic status and NTR expression level in cells, *C. elegans* and tumor tissues.

We fabricated a novel probe, composed of a typical donor- π -acceptor featured chromophore, dicyanomethylene-4H-pyran (DCM), and a nitrobenzene group, to sensitively monitor the NTR level. The elongated conjugated system and asymmetric structure result in a push-pull construction that allows the designed sensor to have a stronger fluorescence signal, and shorter emission wavelength in the presence of NTR when compared to control conditions in which NTR is not present. In this article, we present the synthesis and optical properties of a novel NTR sensitive probe (1). We demonstrated that probe (1) could selectively and accurately

¹College of Chemical Science and Engineering, Yunnan University, Kunming, 650091, PR China. ²Institute of Life Sciences, Yunnan University, Kunming, 650000, China. ³College of Chemistry and Chemical Engineering, Yunnan Normal University, Kunming, 650500, PR China. Correspondence and requests for materials should be addressed to Y.Z. (email: yingzhou@ynu.edu.cn) or J.F.Z. (email: junfengzhang78@aliyun.com)

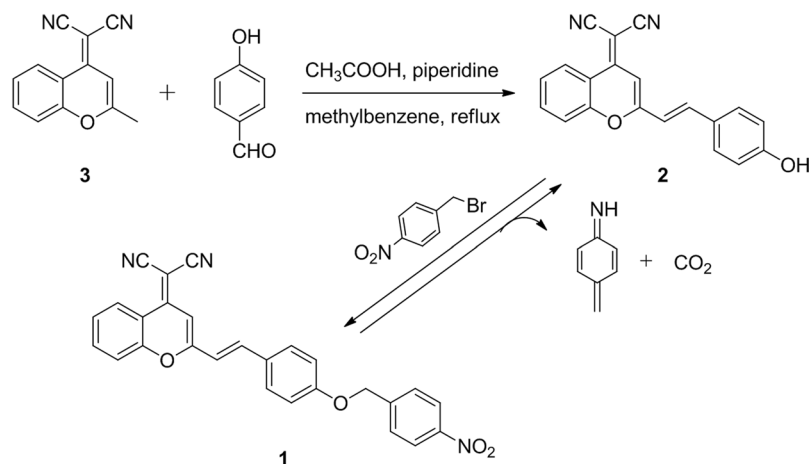


Figure 1. Synthetic route of probe (1), and the reactivity of probe (1) with nitroreductase.

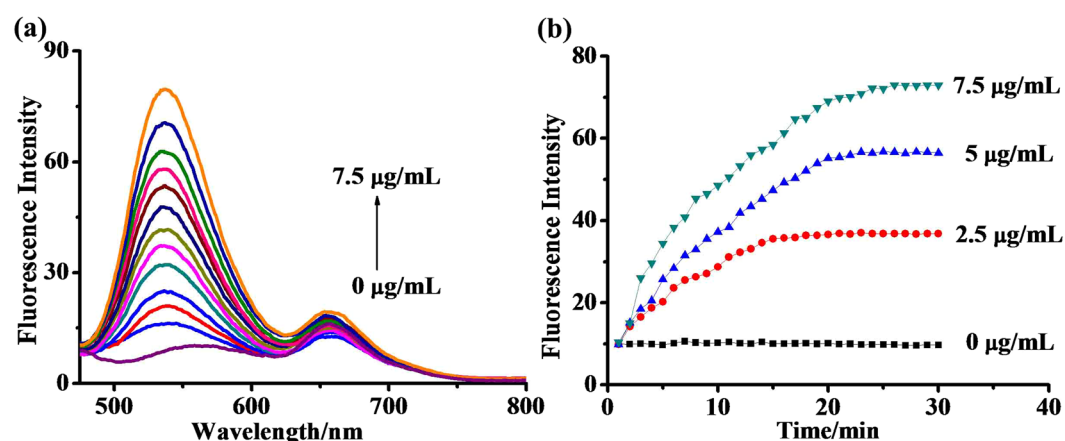


Figure 2. (a) Fluorescence responses of probe (1) (1.0×10^{-5} M) to different concentrations of nitroreductase (NTR) in PBS buffer with 1% DMSO and $10 \mu\text{M}$ NADH. (b) A plot showing the fluorescence intensity of probe (1) (1.0×10^{-5} M) at 537 nm vs. the reaction time in the presence of different concentration of NTR: 0 (control), 2.5, 5, and 7.5 $\mu\text{g/mL}$. Measurements were performed in 10 mM PBS buffer at 37°C (pH = 7.4).

measure endogenous and exogenous NTR levels from different sources with a unique fluorescence enhancement and a large blue-shift. Thus, probe (1) maybe a promising tool for monitoring intracellular hypoxic levels, and maybe used for measuring the hypoxic state in tumors.

Results and Discussion

Synthesis of probe (1). Compound 3, synthesized as previously described²¹, reacted with 4-hydroxybenzaldehyde to generate intermediate compound 2²². Subsequently, intermediate 2 underwent a condensation reaction under relatively mild conditions to form probe (1) (Fig. 1). Synthetic details and characterization of the newly derived probe (1) can be found in the ESI.

Fluorescence responses of probe (1) with NTR. To set up the experimental conditions, we compared the effect of the pH on the emission of 1 versus emission spectra of the reaction of probe (1) catalyzed by NTR. (Fig. S2). Because probe (1) was stable and reduced well by NTR under physiological conditions, pH and temperature conditions were chosen as pH 7.4 and 37°C . The absorption and emission spectra of probe (1) (2.0×10^{-5} M) in the presence and absence of NTR were evaluated in a DMSO/PBS buffer (0.01 M, pH 7.4) (1:99 v/v). Probe (1) exhibited broad absorption in the range of 360–520 nm. The reduction of probe (1) catalyzed by NTR resulted in a decrease of the absorption peak at 345 nm (Fig. S3, ESI). The fluorescent probe itself showed a very weak emission at 660 nm, and the addition of NTR and NADH to the solution of 1, led to an 11-fold increase in fluorescence enhancement at a wavelength of 537 nm. The fluorescence responses of probe (1) to NTR at different concentrations are shown in Fig. 1a. Increasing NTR concentrations showed a gradual increase in fluorescence intensity at 537 nm, the lowest detectable concentration of NTR being 24.5 ng/mL (Fig. S5). The kinetic curves of the fluorescence intensities of probe (1) reacting with different concentrations of NTR resulted in a plateau level (Fig. 2b). The plateau was reached roughly 24 min into the reaction using 7.5 $\mu\text{g/mL}$ NTR.

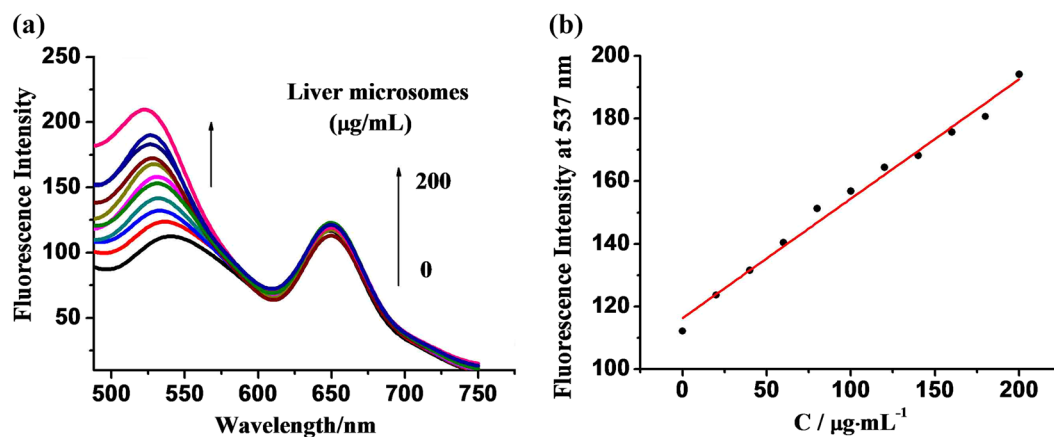


Figure 3. (a) Fluorescence emission titration spectra of probe (1) (3.0×10^{-5} M) in the presence of varying concentrations of rat liver microsome (0~200 $\mu\text{g/mL}$) in PBS (0.01 M, pH = 7.4) with 1% DMSO and 80 μM NADH. (b) Correlation between emission intensities at 537 nm and concentrations of liver microsome.

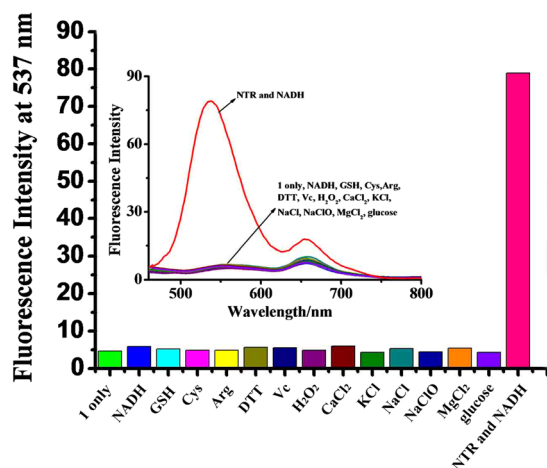


Figure 4. Fluorescence activities of probe (1) (1.0×10^{-5} M) to various species: probe (1) only, NADH (10 μM), GSH (1 mM), Cys (1 mM), Arg (1 mM), DTT (1 mM), Vc (1 mM), H_2O_2 (1 mM), CaCl_2 (1 mM), KCl (1 mM), NaCl (1 mM), NaClO (1 mM), MgCl_2 (1 mM), glucose (1 mM), nitroreductase, and NADH. All measurements were performed in PBS (0.01 M, pH 7.4) with 1% DMSO.

Fluorescence responses of probe (1) reacted with rat liver microsomes. Tang *et al.* were the first to use the rat liver microsome as a source of NTR to test the probe's response²³. Inspired by their work, we tested the optical spectra of probe (1) towards NTR derived from the rat liver microsome. As shown in Fig. 3a, probe (1) itself showed a weak emission at a wavelength of 650 nm. The addition of rat liver microsome to probe (1) resulted in an additional emission peak at roughly 537 nm. A linear relation in fluorescence intensity was obtained at 537 nm using a NTR concentration in the range of 0–200 $\mu\text{g/mL}$ (Fig. 3).

The selectivity of probe (1). The selectivity of probe (1) was determined in comparison with various analytes, such as glutathione (GSH), cysteine (Cys), dithiothreitol (DTT), arginine (Arg), ascorbic acid (Vc), H_2O_2 , NaClO, CaCl_2 , KCl, NaCl, MgCl_2 , glucose, NADH, and NTR with NADH (Fig. 4). We demonstrated that thiol-containing substrates, inorganic salts, and other species total above show no interference with the reaction between probe (1) and NTR, indicating a high selectivity of probe (1) for the detection of NTR in the test condition. The selectivity of NTR detection is provided by the nitrobenzene group in probe (1) (Fig. 1). The mechanism of probe (1) reduction catalyzed by NTR supporting the results of the selectivity tests was confirmed by mass spectrometry analysis of the reaction products (Fig. S6).

The cytotoxicity of probe (1). A low cytotoxicity is a guarantee for the probe's safe applications in *in vitro* and *in vivo* testing. Cytotoxicity of compound 1 was determined by Cell Counting Kit-8 (CKK-8) assays in two control cell lines (MA104 and Ins-1) and two cancer cell lines (A549, SKOV). As shown in Fig. S7, the EC50 values of the control cells (MA104 (33.7 μM); Ins-1 (71.04 μM)) are higher compared to the EC50 values of the

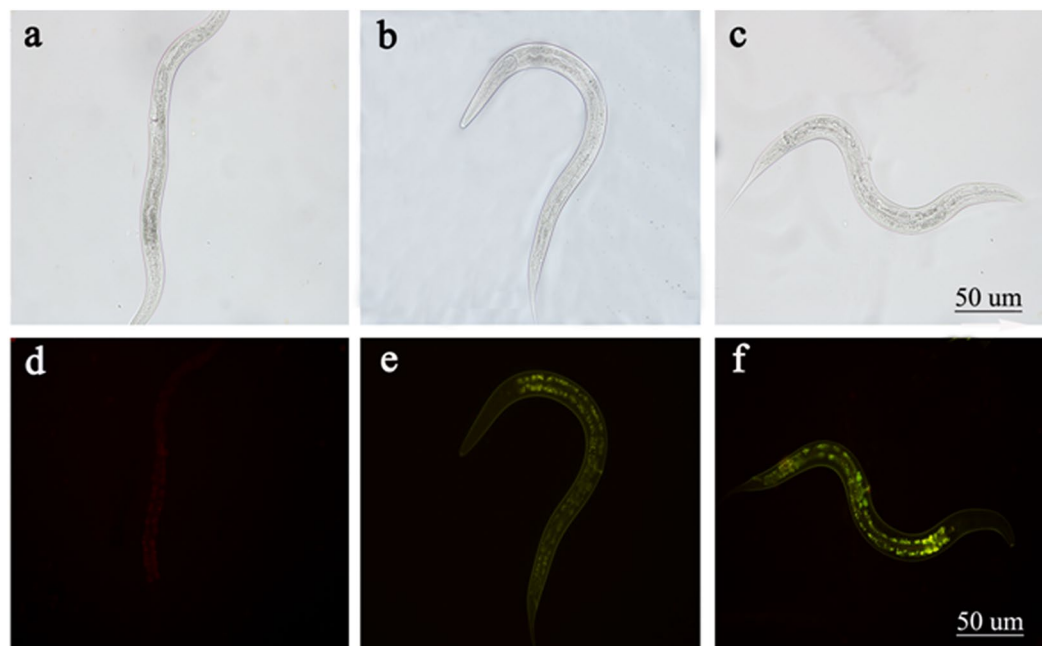


Figure 5. Bright-field image (top) and fluorescent image (bottom) in *C. elegans*. (a) Probe (1) (20 μ M) only. (b) Probe (1) (20 μ M), NADH (100 μ M), and nitroreductase (NTR) (10 μ g/ml). (c) Probe (1) (20 μ M), NADH (100 μ M), and NTR (20 μ g/ml).

cancer cells (A549 (2.7 μ M), SKOV (1.18 μ M)). Thus, the low cytotoxic characteristics of probe (1) indicated its safe potential for *in vivo* measurement of NTR levels.

***In vivo* imaging of probe (1).** The sensitivity of probe 1 was evaluated in *C. elegans* larvae at developmental stage 3 (L3). The larvae were alive and active during exposure to probe (1), indicating the low levels of toxicity of probe (1). To detect exogenous NTR levels in live animals using probe (1), larvae were first incubated in Petri dishes filled with M9 buffer, containing 20 μ M 1 for 1 h at 37 $^{\circ}$ C (Fig. 5a,d). Subsequently, 10 or 20 μ g/mL NTR and 100 μ M NADH was added to the larvae followed by incubation for 1 h at 37 $^{\circ}$ C.

Until addition of NTR (10 μ g/ml) and the second substrate (100 μ M of NADH), no fluorescence was observed in the pre-treated nematodes. However, addition of 20 μ g/ml of NTR, and 100 μ M of NADH resulted in a clear bright green fluorescence signal was emitted from the intestinal region, and gonads of larvae, indicating that probe (1) can visualize the detection of exogenous NTR in *C. elegans*.

Fluorescent imaging of Hi5 cells treated with probe (1) and DAPI, a commercial nuclei dye, was performed to evaluate the potential of probe (1) to penetrate into live cells. Under normoxic conditions, Hi5 cells were incubated for 2 h at 37 $^{\circ}$ C with 20 μ M of probe (1), then nuclei were stained with 1 μ M DAPI for 5 min at 37 $^{\circ}$ C. As shown in Fig. 6, a very weak green fluorescence signal was released from the cytoplasm from cells that were incubated with probe (1). Treatment of the cells with the antioxidant (Glutathione ethyl ester) at different concentrations (0.6 or 1.2 mg/mL) results in a significant decrease in oxygen level. The fluorescence intensity of the probe in the cultured cells increased with the increase of antioxidant concentration. The brightest emission was observed at an antioxidant concentration of 1.2 mg/mL. Thus, the fluorescence intensity of probe (1) correlated with the intracellular redox status of Hi5 cells. Our data suggested that our approach may be used for the detection of hypoxia-induced NTR expression in tumor cells and tissues.

In solid tumors, the level of hypoxia increased with increasing tumor size and correlated with NTR over-expression. Therefore, we hypothesized that probe (1) with NTR as a target may evaluate the hypoxia levels in tumor tissues. To explore the diagnostic potential of our approach, a tumor model was established in which HEPG-2 cell (1×10^7 /mL) in 100 μ L PBS were subcutaneously injected into the left flank of the mice. When the tumor volume reached 1 cm³, mice were sacrificed by cervical vertebra dislocation, and organs including lung, liver, kidney, spleen, intestine, heart and tumors were collected for organ imaging. After 5 h of incubation with 100 μ M of probe (1) at 37 $^{\circ}$ C under hypoxic conditions (5% O₂), tumor tissue demonstrated a strong fluorescence signal when compared to the surrounding tissues (Fig. 7a). Tumor tissue morphology was confirmed by H&E staining (Fig. 7c,d). Immunofluorescence staining using Glypican-3 as a marker of liver cancer, was used for tumor identification (Fig. 7e). And showed that probe (1) could successfully be used to characterize hypoxic tumors. Thus, we demonstrated that probe (1) may be applied as a selective and sensitive bioimaging probe in a mouse model of hypoxic tumors.

In summary, we have successfully developed probe (1), a NTR-targeted fluorescent probe that detects hypoxic conditions in tumor cells and tissues. Our approach is based on the ability of NTR to catalyze the reduction of probe (1) with outstanding sensitivity and selectivity. Probe (1) was used for detecting exogenous NTR in *C. elegans*, and the hypoxic status in Hi5 cells. Moreover, in mice bearing HEPG-2 induced tumors, we demonstrated

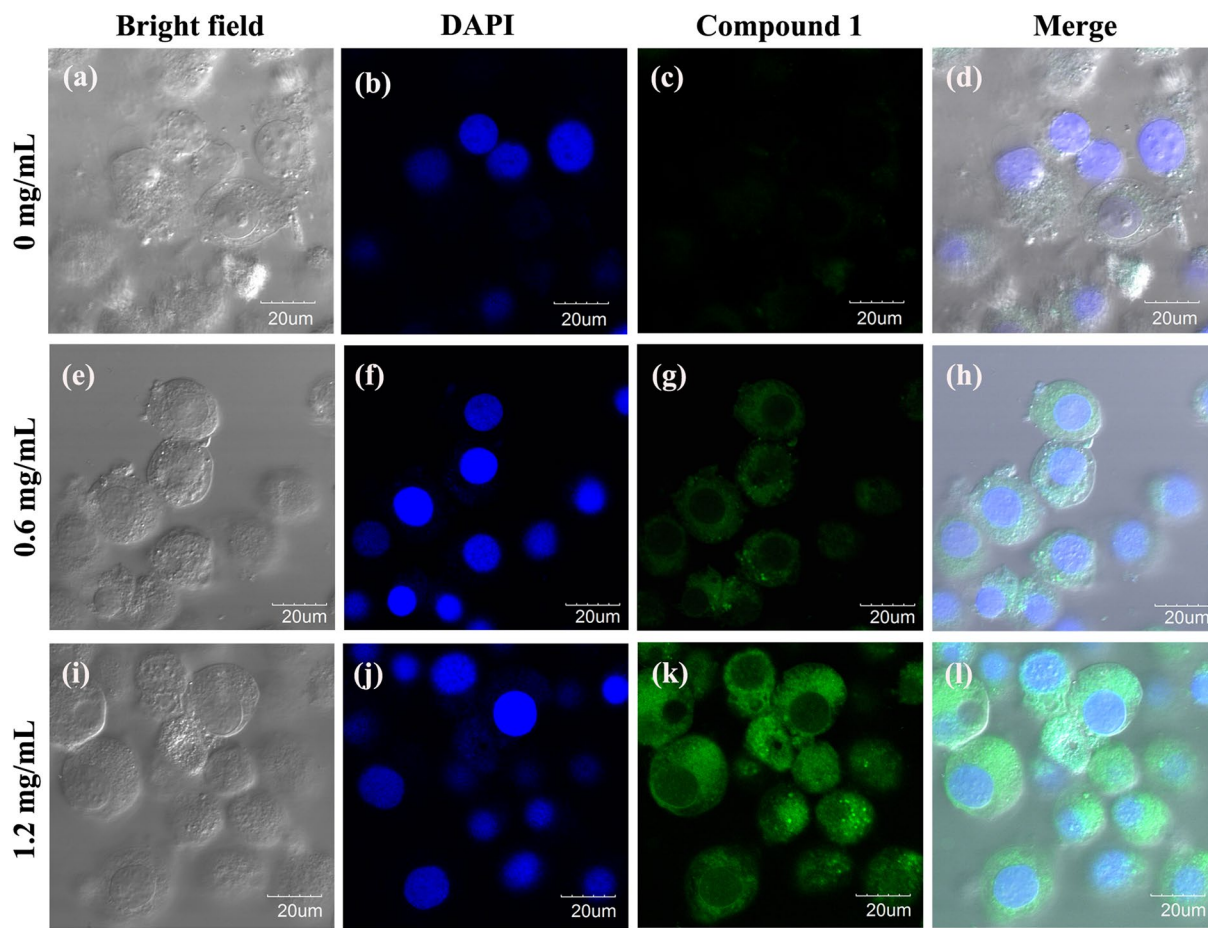


Figure 6. Confocal luminescence images of live Hi5 cells, incubated in PBS for 2 h, at different oxygen levels. (a–d) Probe (1) only (20 μ M); (e–h) Probe (1) (20 μ M), and antioxidant (0.6 mg/mL); (i–l) Probe (1) (20 μ M), and antioxidant (1.2 mg/mL). (a,e) and (i) Are bright-field images. (b,f) and (j) Are blue channels collected at 425–475 nm, stained with DAPI. (c,g) and (k) are green channels collected at 495–550 nm, stained with probe 1. (d,h and l) Are merged images.

that probe (1) is a useful tool for the detection of hypoxic conditions in tumortissue. We anticipate that the application of probe (1) will reveal the bio-roles of NTR, and the relation of NTR and hypoxia in pathological processes.

Methods

All methods were performed in accordance with the relevant guidelines and regulations.

Synthesis of probe (1). (For detailed synthetic procedures, please see the Supporting Information.) A mixture of compound 2 (0.2 g, 0.64 mmol), 1-(bromomethyl)-4-nitrobenzene (0.166 g, 0.768 mmol), K_2CO_3 (0.442 g, 3.2 mmol), and NaI (0.048 g, 0.32 mmol) in 25 mL CH_3COCH_3 were heated under reflux for 4 h. After completion of the reaction, the mixture was cooled to room temperature, and condensed under reduced pressure. Chromatography of the crude product on silica gel using CH_2Cl_2 as an eluent resulted in a pale reddish orange solid product of 258.3 mg (yield = 90%). 1H NMR (500 MHz, $DMSO-d_6$) δ (ppm): 8.69 (d, 1H), 8.27–8.26 (d, 2H), 7.91(d, 1H), 7.77–7.69 (d, 6H), 7.59 (d, 1H), 7.36–7.33 (d, 1H), 7.13–7.12 (d, 2H), 6.95 (d, 1H), 5.34 (s, 2H). ^{13}C NMR (125 MHz, $DMSO-d_6$) δ (ppm):160.18, 158.91, 153.32, 152.41, 147.45, 144.99, 138.85, 135.75, 130.47, 128.67, 126.50, 125.01, 124.02, 119.41, 117.82, 117.65, 117.49, 116.32, 115.86, 106.54, 68.59, 60.03.

Preparation of the test solution. PBS(pH = 7.4), and analyticalgrade DMSO were used for spectroscopic studies. The probe 1 stock solution (1×10^{-3} mol/L) was prepared in analyticalgrade DMSO. The concentration of probe (1) in test solution was 1×10^{-5} mol/L, and was prepared by mixing 50 μ L stock solution and 4.95 mL PBS. Then 10 μ L NADH, and increasing concentrations of NTR (0, 2.5, 5, and 7.5 μ g/mL) were added to the test solution. For selectivity studies, various analytes, including glutathione (GSH), cysteine (Cys), dithiothreitol (DTT), arginine (Arg), ascorbic acid (Vc), H_2O_2 , NaClO, $CaCl_2$, KCl, NaCl, $MgCl_2$, glucose, NADH, and NTR were added to probe (1).

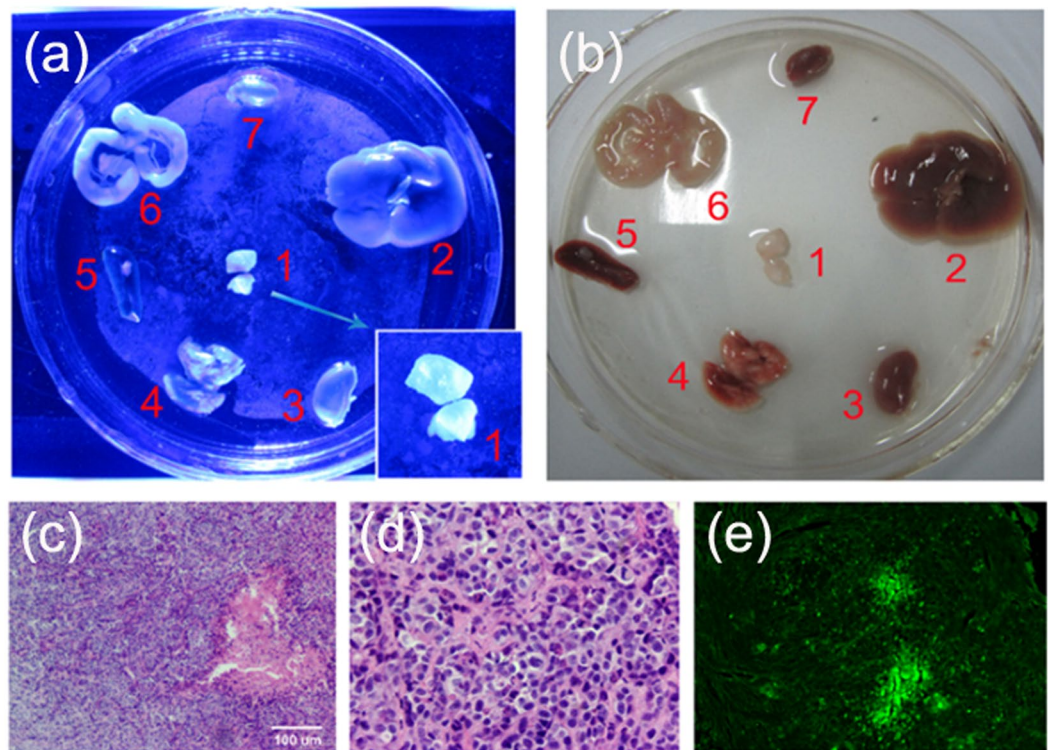


Figure 7. (a) and (b) Representative images of dissected organs of a mouse bearing HEPG-2-induced tumors. The mouse was sacrificed and organs were removed and incubated with $100\ \mu\text{M}$ of 1 for 5 hours under hypoxic conditions. 1. HEPG-2 tumor; 2. lung; 3. liver; 4. kidney; 5. spleen; 6. intestine; 7. heart. (c) H&E staining of murine sarcoma HEPG-2-induced tumor ($\times 100$). (d) H&E staining of murine sarcoma HEPG-2-induced tumor ($\times 400$). (e) Immunofluorescence of HEPG-2 tumor by Glypican 3 staining.

Cytotoxicity assays. To investigate the cytotoxicity of probe (1), CCK-8 tests were performed in A549 and SKOV cancer cells, and MA104 and Ins-1 control cells. Cells were seeded into 96-well microplates with $90\ \mu\text{L}$ of cell suspension, and cells were incubated for 24 hours at $37\ ^\circ\text{C}$ under $5\% \text{CO}_2$. Cells were washed, followed by addition of increasing concentrations ($0.1\ \mu\text{M}$ – $10\ \mu\text{M}$) of probe 1. After 24 h, $10\ \mu\text{L}$ of CCK solution was added to each well, followed by incubation for 2–3 hours at $37\ ^\circ\text{C}$. Absorbance was read at $450\ \text{nm}$ using a microplate reader (Thermo Multiscan Go).

Cell culture. Hi5 cells were kindly provided by the institute of life sciences, Yunnan University. Cells were maintained in Dulbecco's modification Eagle's medium (DMEM, Invitrogen) supplemented with 10% fetal bovine serum (FBS) at $37\ ^\circ\text{C}$ and $5\% \text{CO}_2$. The cells were seeded in a confocal dish, and incubated for 24 h at $37\ ^\circ\text{C}$ at $5\% \text{CO}_2$. Then the cells were incubated with $20\ \mu\text{M}$ probe (1), and different concentrations of the antioxidant ($0\ \text{mg}/\text{mL}$, $0.6\ \text{mg}/\text{mL}$, $1.2\ \text{mg}/\text{mL}$) for 2 h at $37\ ^\circ\text{C}$ in $5\% \text{CO}_2$.

C. elegans culture. The *C. elegans* wild type strain N_2 was acquired from the institute of life sciences, Yunnan University. *C. elegans* in the larval stage 4 (L4) were incubated at $20\ ^\circ\text{C}$ for 1 h in Petri dishes filled with M9 buffer, containing probe (1) ($20\ \mu\text{M}$). After incubation, the exposed nematodes were washed three times with M9 buffer and centrifuged at $3000\ \text{r}/\text{min}$ for 2 minutes. Then NADH ($100\ \mu\text{M}$), and different concentrations of NTR ($0\ \mu\text{g}/\text{mL}$, $10\ \mu\text{g}/\text{mL}$, and $20\ \mu\text{g}/\text{mL}$) were added to the nematode. Images of the mounted nematodes were acquired by a fluorescent microscopy Olympus BX51.

Co-staining of cells. To confirm that probe (1) specifically stained the cytoplasm where NTR is mainly generated, co-staining studies were performed. Under normoxic conditions, Hi5 cells were incubated with $20\ \mu\text{M}$ of probe (1) for 2 h at $37\ ^\circ\text{C}$. Under hypoxic conditions, antioxidant (Glutathione ethyl ester) at different concentrations (0.6 or $1.2\ \text{mg}/\text{mL}$) was added and nuclei were stained for 5 min with $1\ \mu\text{M}$ DAPI. Emission was analyzed using blue channels and a wavelength of 425 – $475\ \text{nm}$ for DAPI, and green channels at 495 – $550\ \text{nm}$ for probe (1). Fluorescence imaging was performed using an Olympus FV1000 confocal microscopy with a $40\times$ objective lens.

Establishing a human hepatoma tumor-bearing nude mouse model. All procedures involving animals were approved by the Committee on the Use of Live Animals in Teaching and Research of Yunnan Minzu University. Female SPF nude mice (weighing 16 – $20\ \text{g}$) were randomly divided into two experimental groups. To establish a human hepatoma tumor model, $1 \times 10^7/\text{mL}$ HEPG-2 cells were diluted with $100\ \mu\text{L}$ PBS, and subcutaneously injected into the right armpit of the mice. Weights were measured and general behavior and body

condition was assessed. On day 21 after injection, all mice were sacrificed, and tumors were isolated and measured by Vernier caliper to calculate tumor volume ($V = a \times b^2/2$).

Immunohistochemistry. Tissues were fixed for 48 h in 4% formalin, and dehydrated in a graded series of ethanol. Tissues were embedded in paraffin and sliced into 4 μm sections. Subsequently, sections were deparaffinized, and stained with hematoxylin and eosin (HE) for histological analysis. After dewaxing and dehydration, sections were washed 3 \times 5 min with distilled water. Then the sections were boiled in citrate buffer solution for 30 min, followed by washing in PBS for 3 \times 5 min. The sections were incubated for 30 min in 10% serum at 37 °C. Serum was removed, and a rabbit-anti mouse monoclonal anti-Glypican 3 antibody (1:1,000, Abcam, MA, USA) was added to each well, and incubated overnight at 4 °C. After rinsing with PBS, sections were incubated with a FITC-conjugated goat-anti rabbit antibody (1:2,000, Abcam). After another incubation for 2 h at 37 °C, the sections were washed with PBS for 3 \times 5 min. Then sections were examined under a fluorescence microscope (Leica DMI3000B, Leica Microsystems Ltd., Wetzlar, Germany) using a mercury laser to excite FITC at 488 nm. Emission was recorded at 525 nm.

The anti-HIF1 α antibody (CST, MA, USA; 1:100 dilution) was used for immunohistochemistry (IHC) after validation and optimization. IHC was performed according to published protocols²⁴, with a standard diaminobenzidine (DAB) staining protocol. Briefly, antigens were first retrieved by boiling the slides in 0.1 M Tris-HCl (pH 9.0) buffer for 5 min. After washing with 0.1 M PBS containing 0.1% Triton X-100, slides were then incubated with the anti-HIF1 α primary antibody at 4 °C overnight. Then the biotinylated anti-mouse secondary antibody and the avidin-biotin complex (Vector Laboratories, Burlingame, USA) were applied to the slides sequentially. Finally, slides were incubated with DAB (Vector Laboratories) until suitable staining developed.

References

- Palmer, B. D., Zijl, P. V., Denny, W. A. & Wilson, W. R. Reductive Chemistry of the Novel Hypoxia-Selective Cytotoxin 5-[N,N-Bis(2-chloroethyl)amino]-2,4-dinitrobenzamide. *J Med Chem* **38**, 1229–1241, doi:10.1021/jm00007a019 (1995).
- Bae, J. *et al.* Nitroreductase-triggered activation of a novel caged fluorescent probe obtained from methylene blue. *Chem Comm* **51**, 12787–12790, doi:10.1039/C5CC03824C (2015).
- Wong, R. H., Kwong, T., Yau, K. H. & Au-Yeung, H. Y. Real time detection of live microbes using a highly sensitive bioluminescent nitroreductase probe. *Chem Comm* **51**, 4440–4442, doi:10.1039/C4CC10345A (2015).
- Zhang, J. *et al.* Efficient Two-Photon Fluorescent Probe for Nitroreductase Detection and Hypoxia Imaging in Tumor Cells and Tissues. *Anal Chem* **87**, 11832–11839, doi:10.1021/acs.analchem.5b03336 (2015).
- Kiyose, K. *et al.* Hypoxia-Sensitive Fluorescent Probes for *in Vivo* Real-Time Fluorescence Imaging of Acute Ischemia. *J Am Chem Soc* **132**, 15846–15848, doi:10.1021/ja105937q (2010).
- Cui, L. *et al.* New Prodrug-Derived Ratiometric Fluorescent Probe for Hypoxia: High Selectivity of Nitroreductase and Imaging in Tumor Cell. *Org Lett* **13**, 928–931, doi:10.1021/ol102975 (2011).
- Li, Y. *et al.* Ultrasensitive near-infrared fluorescence-enhanced probe for *in vivo* nitroreductase imaging. *J. Am. Chem. Soc J Am Chem Soc* **137**, 6407–6416, doi:10.1021/jacs.5b04097 (2015).
- Zhou, Y. & Yoon, J. Recent progress in fluorescent and colorimetric chemosensors for detection of precious metal ions (silver, gold and platinum ions). *Chem Soc Rev* **41**, 52–67, doi:10.1039/C1CS15159B (2012).
- Zhou, Y., Zhang, J. F. & Yoon, J. Fluorescence and colorimetric chemosensors for fluoride-ion detection. *Chem Rev* **114**, 5511–5571, doi:10.1021/cr400352m (2014).
- Chinen, A. B. *et al.* Nanoparticle Probes for the Detection of Cancer Biomarkers, Cells, and Tissues by Fluorescence. *Chem. Rev* **115**, 10530–10574, doi:10.1021/acs.chemrev.5b00321 (2015).
- Chen, X. Q. *et al.* Recent progress in the development of fluorescent, luminescent and colorimetric probes for detection of reactive oxygen and nitrogen species. *J Chem Soc Rev* **45**, 2976–3016, doi:10.1039/C6CS00192K (2016).
- Lee, M. H. *et al.* Mitochondrial thioredoxin-responding off-on fluorescent probe. *J Am Chem Soc* **134**, 17314–17319, doi:10.1021/ja308446y (2012).
- Lee, M. H. *et al.* Mitochondria-immobilized pH-sensitive off-on fluorescent probe. *J Am Chem Soc* **136**, 14136–14142, doi:10.1021/ja506301n (2014).
- Xiao, H., Li, P., Zhang, W. & Tang, B. An ultrasensitive near-infrared ratiometric fluorescent probe for imaging mitochondrial polarity in live cells and *in vivo*. *Chem Sci* **7**, 1588–1593, doi:10.1039/C5SC04099J (2016).
- Miao, J. F. *et al.* Fast-response and highly selective fluorescent probes for biological signaling molecule NO based on N-nitrosation of electron-rich aromatic secondary amines. *Biomaterials* **78**, 11–19, doi:10.1016/j.biomaterials.2015.11.011 (2016).
- Yu, F. B., Gao, M., Li, M. & Chen, L. X. A dual response near-infrared fluorescent probe for hydrogen polysulfides and superoxide anion detection in cells and *in vivo*. *Biomaterials* **63**, 93–101, doi:10.1016/j.biomaterials.2015.06.007 (2015).
- Xue, C., Lei, Y. J., Zhang, S. C. & Sha, Y. W. A. cyanine-derived “turn-on” fluorescent probe for imaging nitroreductase in hypoxic tumor cells. *Anal Methods* **7**, 10125–10128, doi:10.1039/C5AY02312B (2015).
- Xu, J. *et al.* A rapid response “Turn-On” fluorescent probe for nitroreductase detection and its application in hypoxic tumor cell imaging. *Analyst* **140**, 574–581, doi:10.1039/C4AN01934B (2015).
- Li, Z. *et al.* *in vivo* imaging and detection of nitroreductase in zebrafish by a new near-infrared fluorescence off-on probe. *Biosensors and Bioelectronics* **63**, 112–116, doi:10.1016/j.bios.2014.07.024 (2015).
- Shi, Y. M., Zhang, S. C. & Zhang, X. R. A novel near-infrared fluorescent probe for selectively sensing nitroreductase (NTR) in an aqueous medium. *Analyst* **138**, 1952–1955, doi:10.1039/C3AN36807F (2013).
- Xu, K. H. *et al.* A two-photon fluorescent probe with near-infrared emission for hydrogen sulfide imaging in Biosystems. *Chem. Comm* **49**, 3890–3892, doi:10.1039/C3CC41244J (2013).
- Li, M. *et al.* A near-infrared colorimetric fluorescent chemodosimeter for the detection of glutathione in living cells. *Chem Comm* **50**, 1751–1753, doi:10.1039/C3CC48128J (2014).
- Sun, W. *et al.* High selectivity imaging of nitroreductase using a near-infrared fluorescence probe in hypoxic tumor. *Chem Comm* **49**, 2554–2556, doi:10.1039/C3CC38980D (2013).
- Liu, R., Zhou, Z., Huang, J. & Chen, C. PMEPA1 promotes androgen receptor-negative prostate cell proliferation through suppressing the Smad3/4-c-Myc-p21 Cip1 signaling pathway. *J Pathol.* **223**, 683–694, doi:10.1002/path.2834 (2011).

Acknowledgements

This work was supported by the Natural Science Foundation of China (21262045, 21262050, 21302165, 21462050 and 21672185), the Foundation of the Department of Science and Technology of Yunnan Province of China (2013HB062, 2014HB008, 2016FB020), the Youth Talent Training Program of Yunnan University (WX173602).

Author Contributions

Y.Z. and J.F.Z. conceived the idea and directed the work. D.Y. performed the main synthesis and the *in vitro* and *in vivo* fluorescence tests. T.N.Z. tested some *in vitro* fluorescence tests. M.L. and H.Y.T. provided the materials of biological experiments and performed some biological tests.

Additional Information

Supplementary information accompanies this paper at doi:[10.1038/s41598-017-09525-2](https://doi.org/10.1038/s41598-017-09525-2)

Competing Interests: The authors declare that they have no competing interests.

Publisher's note: Springer Nature remains neutral with regard to jurisdictional claims in published maps and institutional affiliations.



Open Access This article is licensed under a Creative Commons Attribution 4.0 International License, which permits use, sharing, adaptation, distribution and reproduction in any medium or format, as long as you give appropriate credit to the original author(s) and the source, provide a link to the Creative Commons license, and indicate if changes were made. The images or other third party material in this article are included in the article's Creative Commons license, unless indicated otherwise in a credit line to the material. If material is not included in the article's Creative Commons license and your intended use is not permitted by statutory regulation or exceeds the permitted use, you will need to obtain permission directly from the copyright holder. To view a copy of this license, visit <http://creativecommons.org/licenses/by/4.0/>.

© The Author(s) 2017